The Astrophysical Journal, 579:626–638, 2002 November 10

THORIUM AND URANIUM CHRONOMETERS APPLIED TO CS 31082-001

Hendrik Schatz,[1,2] Ralf Toenjes,[1,2] Bernd Pfeiffer,[3] Timothy C. Beers,[2] John J. Cowan,[4]
Vanessa Hill,[5] and Karl-Ludwig Kratz[3]
Received 2002 March 6; accepted 2002 July 17

ABSTRACT

We use the classical *r*-process model to explore the implications of the recently reported first observation of U in the extremely metal-poor, *r*-process element–enriched halo star CS 31082-001 for U and Th cosmochronometry. Using updated nuclear physics input and performing a new, conservative, analysis of the remaining uncertainties in the classical *r*-process model, we confirm that U (together with Th) abundance observations in metal-poor stars are a promising tool for dating *r*-process events in the early Galaxy, independent of assumptions on Galactic chemical evolution. We show that nuclear physics uncertainties limit the present accuracy of estimated U/Th ages to about 2 Gyr. Critical nuclear data that are required to lower this uncertainty include β-delayed fission branchings and reliable predictions of the onset of deformation in the vicinity of the $N = 184$ shell closure around ^{244}Tl, as both directly affect predicted U/Th ratios in *r*-process models. In this paper we apply, for the first time, the new HFBCS-1 mass model within the framework of the classical *r*-process model. We find that the predicted U and Th abundances are incompatible with the solar U and Th abundances and trace this back to a different prediction of the onset of deformation around ^{244}Tl. In the case of CS 31082-001, we find it likely that the zero-age U and Th abundances were enhanced by about a factor of 2.5 compared to both (1) a theoretical extrapolation from the observed stable elements using the classical *r*-process model and (2) the zero-age abundances of Th and U in other *r*-process–enhanced, metal-poor halo stars. Although presently ad hoc, this "actinide boost" assumption solves the apparent problem of the relative age difference compared with other metal-poor halo stars and, at the same time, the problem of the inconsistency of ages based on U/(stable nucleus), Th/(stable nucleus) and U/Th ratios. There clearly exist differences, among some *r*-process–enhanced, metal-poor stars, in the level of the elemental abundances of actinides beyond the third *r*-process peak. Whether CS 31082-001 is a relatively rare case or commonplace awaits the identification of larger numbers of *r*-process–enhanced, metal-poor stars in which both U and Th can be measured. Using the U/Th ratio, we obtain a best age estimate for the *r*-process elements in CS 31082-001 of 15.5 ± 3.2 Gyr. Future observations of Pb and Bi and a better determination of the *r*-process contribution to solar Pb are needed to put the age estimates for this and other stars on a more solid basis. For our most likely scenario, we provide predictions of the expected upper and lower limits on the abundances of the elements Pb and Bi in CS 31082-001.

Subject headings: Galaxy: abundances — Galaxy: evolution — nuclear reactions, nucleosynthesis, abundances — stars: abundances — stars: Population II

1. INTRODUCTION

Stellar elemental abundance observations of long-lived radioactive nuclear species synthesized in the *r*-process can be used to derive estimates for the ages and history of the underlying nucleosynthesis events. This method was first applied to stars other than the Sun by Butcher (1987), using Th observations (14 Gyr half-life), and was later extended to very metal-poor stars by François, Spite, & Spite (1993). Since then, such observations have provided considerable information concerning the history of neutron-capture element enrichment in our Galaxy and have placed important constraints on the still unknown site(s) of the *r*-process (see, e.g., Mathews & Cowan 1990; Burris et al. 2000; Kratz et al. 2000a; Pfeiffer et al. 2001). When the observed Th abundance is compared with an *r*-process model prediction, absolute ages of the *r*-process events can be determined as well. This is especially interesting for very metal-poor stars, where this method can provide a useful limit on the age of the Galaxy, independent of chemical evolution models. This application was first done, by Cowan et al. (1997), for the extremely metal-poor giant CS 22892-052, a star that, despite its overall low metallicity ([Fe/H] = −3.1), is extremely enriched in *r*-process elements (e.g., *r*-process/Fe of ≈40 times solar). The method was later refined by Cowan et al. (1999) and applied to other stars as well.

An important assumption underlying all Th cosmochronometry applications is that all *r*-process events produce the *same* relative abundance pattern among the heavier species, especially the same ratio of Th to a stable rare earth reference element, often taken to be Eu. Many earlier studies of the elemental abundances of metal-poor stars suggested that, indeed, the abundance patterns for many such stars do resemble a solar *r*-process pattern (Spite & Spite 1978;

[1] National Superconducting Cyclotron Laboratory, Michigan State University, East Lansing, MI 48824; schatz@nscl.msu.edu, toenjes@nscl.msu.edu.
[2] Department of Physics and Astronomy, Michigan State University, East Lansing, MI 48824; beers@pa.msu.edu.
[3] Institut für Kernchemie, Universität Mainz, D-55128 Mainz, Germany; pfeiffer@vkcmzd.chemie.uni-mainz.de, klkratz@mail.kernchemie.uni-mainz.de.
[4] Department of Physics and Astronomy, University of Oklahoma, Norman, OK 73019; cowan@nhn.ou.edu.
[5] European Southern Observatory, D-85748 Garching, Germany; Vanessa.Hill@obspm.fr.

Burris et al. 2000 and references therein). A breakthrough came with the high-quality abundance data for CS 22892-052 (Sneden et al. 1994; McWilliam et al. 1995a, 1995b; Cowan et al. 1995; Sneden et al. 1996; Cowan et al. 1999; Sneden et al. 2000a), in which nearly perfect agreement between the observed stellar and solar system *r*-process abundance pattern could be demonstrated for 18 nuclei with $Z > 55$. The stability of the *r*-process abundance pattern among different *r*-process events was later confirmed by the observation of the same solar pattern for additional metal-poor stars, e.g., HD 126238 (Cowan et al. 1999; Johnson & Bolte 2001), HD 115444 (Westin et al. 2000), HD 186478, HD 108577, and BD $+08°2548$ (Johnson & Bolte 2001), and BD $+17°3248$ (Cowan et al. 2002), as well as in individual giants in Galactic globular clusters (Sneden et al. 2000b; Johnson & Bolte 2001).

The utility of Th chronometers is strongly limited by the relatively long half-life of ^{232}Th, 14 Gyr; even for relatively accurate abundance data, large errors can result in the derived ages. U, on the other hand, with its much shorter half-life of 4.5 Gyr, could in principle be used to obtain more accurate ages. For many years, the technique of U- and U/Th-based *r*-process cosmochronometry could only be applied to U and Th observations in chemically peculiar stars (Cowley, Allen, & Aikman 1975), or to solar U and Th abundances in connection with Galactic chemical evolution models (see Cowan, Thielemann, & Truran 1991; Meyer & Truran 2000 for reviews). The recent first successful measurement of a U abundance in an extremely metal-poor halo star (CS 31082-001; Cayrel et al. 2001) marks, therefore, a new era in *r*-process cosmochronometry. However, while opening up the possibility of more precise U-based age estimates, the extremely high Th abundance in CS 31082-001 indicates for the first time a possible variation in the zero-age (the time of the *r*-process event) actinide abundances, compared to those of other metal-poor halo stars with large *r*-process element enhancements (Goriely & Arnould 2001; Hill et al. 2002). Nevertheless, Cayrel et al. (2001) provided a first age estimate for CS 31082-001 of 12.5 ± 3.3 Gyr, based on preliminary abundance data (Hill et al. 2001) and previous *r*-process model predictions for the U/Th ratio. Recently, a refined analysis of the CS 31082-001 spectra, using an improved model atmosphere and new experimental oscillator strengths for U II and Th II transitions, has led to significant improvements in the derived elemental abundances (Hill et al. 2002). In addition, Goriely & Arnould (2001) used the "multievent canonical *r*-process model" to obtain new estimates on the *r*-process production of U and Th. With a large variety of nuclear physics input, they find a large variation in the *r*-process production of the actinides. The resulting age range for the *r*-process elements in CS 31082-001 is 9–18 Gyr. Hill et al. (2002) provide an age estimate for this star of 14.0 ± 2.4 Gyr, without taking into account the errors arising from the nuclear physics predictions.

In this paper we take a different approach, based on the classical *r*-process model, to better constrain the *r*-process production of U and Th. This leads to a more meaningful analysis of the implications of the U and Th observations in CS 31082-001, with realistic estimates for all sources of uncertainty. In contrast to the multievent canonical *r*-process model, the additional assumption of a smooth behavior of temperature and neutron density in the *r*-process reduces the number of free parameters considerably. Therefore, all stable *r*-process elements, especially those in the $A = 195$ peak, can serve as constraints for the actinide production in the *r*-process. Details are provided in § 2 below. In § 3, we describe an update of our nuclear physics database for the classical *r*-process model. We then discuss, in § 4, new estimates of the remaining uncertainties in the model predictions for the synthesis of U and Th in the *r*-process.

In § 5, we present an application of this improved model to CS 31082-001, taking full advantage of the existence of three potential chronometer pairs: the abundance ratios Th/X, U/X, and U/Th, where X is a suitable, stable, *r*-process element. Requiring consistency among the different ages is a powerful tool to improve age estimates. If one assumes a solar zero-age abundance distribution, then the consistency requirement for the Th/X, U/X, and U/Th ages can be used to test and constrain the *r*-process model used. The significance of this lies not so much in an improved understanding of the *r*-process as in obtaining a refined *r*-process model that can be used to derive more reliable ages for CS 31082-001 and other stars, including those for which only Th can be observed. If, on the other hand, there is doubt about the existence of a zero-age solar *r*-process abundance pattern, then the consistency of Th/X, U/X, and U/Th ages can be used determine to what extent deviations from a solar abundance pattern affect the predicted zero-age abundances of U and Th. In this case, one relies on the *r*-process model and the associated uncertainty estimates. The age consistency requirement can therefore be used to establish the zero-age abundance pattern beyond Pb, yielding constraints for models attempting to explain a nonsolar distribution and allowing one to extend systematic *r*-process abundance comparisons in metal-poor stars into the actinide region, once a larger sample of stars with observed U abundances becomes available. The latter is the approach we use in this paper, as indeed the abundance data on CS 1082-001 indicate, for the first time, significant differences relative to an extrapolated zero-age solar *r*-process abundance pattern (Goriely & Arnould 2001; Hill et al. 2002).

2. THE *r*-PROCESS MODEL

Determination of absolute ages from the observation of Th or U in metal-poor stars requires prediction of the ^{232}Th and ^{238}U produced in the *r*-process (the zero-age abundances). As the site of the *r*-process has not yet been identified with certainty (nor are we even sure that it can be thought of as a single site; see Sneden et al. 2000a), for our present analysis we employ the so-called classical *r*-process model, a largely model-independent, parameterized approach (Cowan et al. 1991; Kratz et al. 1993; Freiburghaus et al. 1999). This approach has been used extensively in *r*-process cosmochronometry (Pfeiffer, Kratz, & Thielemann 1997; Cowan et al. 1999; Kratz et al. 2000b; Pfeiffer et al. 2001). The calculations are performed within the waiting-point approximation, assuming complete (n, γ)–(γ, n) equilibrium within an isotopic chain, as shown in detail in Freiburghaus et al. (1999). The reaction network can then be reduced to a network of β-decays connecting isotopic chains, while the abundance distribution *within* an isotopic chain is given by the Saha equation and is therefore entirely determined by neutron separation energies for a given temperature T and neutron density n_n (see, e.g., Cowan et al. 1991; Kratz et al. 1993). A single *r*-process component is calculated assuming

irradiation of an Fe seed, with constant neutron number density n_n and constant temperature T, for a time τ. The r-process abundances are then calculated as a superposition of many components, assuming a power-law distribution of the component weights, $\omega(n_n) = a_1 n_n^{a_2}$, and irradiation timescales, $\tau(n_n) = a_3 n_n^{a_4}$, as a function of neutron density. The temperature remains fixed. The number of components is chosen sufficiently high for the final abundances to converge. The nuclei produced in such a calculation are unstable nuclei very far from β^- stability. The final abundances are then calculated in a second step, following all decays of short-lived, unstable nuclei with an α- and β-decay network, including β-delayed emission of up to three neutrons. The processes of β-delayed fission, spontaneous fission, and neutron-capture–induced fission are also taken into account to calculate the final abundance distribution of stable and/or long-lived isotopes.

The critical question for the application of an r-process model for U and Th chronometry is its predictive power beyond the fitted range of stable solar system r-process abundances. Given the large astrophysical uncertainties concerning the r-process site(s), we feel that the classical model is a reasonable choice for the following reasons:

1. The classical r-process model is able to fit the isotopic solar r-process abundance pattern from Fe to Pb with only four free parameters (T and the coefficients a_2, a_3, and a_4; a_1 is a normalization constant), which are adjusted by a least-squares fitting procedure. The small number of free parameters suggests that the general features of this method reflect (possibly in a very indirect way) physical properties of the astrophysical r-process site. This conjecture has been further strengthened by a recent study (Freiburghaus et al. 1999) comparing the classical r-process model with a full dynamic network calculation of a superposition of entropies and electron abundances, reflecting conditions encountered, for example, in the ν-heated, high-entropy bubble above the proto–neutron star in a core-collapse supernova.

2. The classical r-process model is able to reproduce the solar r-process abundances of ^{206}Pb, ^{207}Pb, ^{208}Pb, and ^{209}Bi. This is significant, since more than 80% of the abundance of these species is thought to be produced from α-decay chains originating in the actinide region (Cowan et al. 1999). Pb and Bi isotopes thus serve as a probe for the r-process *in the same region where* U *and* Th *are synthesized* and hence provide a stringent constraint for the extrapolation of r-process models into the actinide region (for a detailed discussion, see Cowan et al. 1999).

3. NUCLEAR PHYSICS

The nuclear physics input needed for the classical r-process model comprises nuclear masses, β-decay rates, branchings for β-delayed neutron emission, and fission barriers to calculate spontaneous fission rates, neutron-induced fission rates, and branchings for β-delayed fission. For the vast majority of these data, no experimental information is available (except for some masses and β-decay properties around ^{80}Zn and ^{130}Cd and some spontaneous fission rates); hence, the model has to rely on theoretical predictions.

The β-decay rates and branchings for β-delayed neutron emission of up to three neutrons used in this work are the same as in Cowan et al. (1999). These are, when no experimental value is available, based on QRPA calculations of the Gamow-Teller (GT) strength function for allowed transitions (see Möller, Nix, & Kratz 1997 and references therein for a description of the method) and an estimate for the first forbidden strength from gross theory (Takahashi, Yamada, & Kondoh 1973). In addition, local nuclear structure systematics, in part based on experimental data, have been taken into account for the theoretical calculations of β-decay properties, following the methods outlined, for example, in Kratz et al. (1993). Test calculations showed that branchings for the emission of more than three neutrons following β-decay are small and therefore are assumed to be of negligible consequence.

Nuclear masses have been taken from two models. The ETFSI-Q model (Pearson, Nayak, & Goriely 1996) takes into account the quenching of neutron shell gaps far from stability, predicted by Hartree-Fock-Bogolyubov calculations (Dobaczewski, Nazarewicz, & Werner 1995). It has been shown that neutron separation energies predicted by the ETFSI-Q mass model yield the best agreement between r-process model predictions and observed abundances (Pfeiffer et al. 1997; Kratz, Pfeiffer, & Thielemann 1998). For comparison, we also performed calculations with the recently developed HFBCS-1 mass model (Goriely, Tondeur, & Pearson 2001). The HFBCS-1 mass model avoids some of the approximations in the ETFSI method (Aboussir et al. 1995), but is essentially based on the same nonrelativistic Hartree-Fock approach with Skyrme forces and Bardeen-Cooper-Schrieffer (BCS) pairing. The HFBCS-1 predictions are therefore similar to the ETFSI-1 predictions (Aboussir et al. 1995; the same model as ETFSI-Q, but without shell quenching), although a slightly improved fit to neutron separation energies has been achieved.

Figure 1 shows the r-process "path" for both mass models, where "path" is defined as the sum of nuclei that β-decay during neutron irradiation for all r-process components used in the calculation. These nuclei are the progenitors that later decay into the stable r-process isotopes. We wish to emphasize that, because of the rapidly changing astrophysical conditions that are expected to apply in nature, there is no single direct r-process path, in the sense of a single reaction sequence of neutron captures and β-decays, that extends from Fe to U. Our r-process path, derived in the classical r-process model, denotes the region of nuclei where a local r-process flow forms the final abundance pattern. It is not necessarily identical with the reaction sequences carrying the r-process into heavier mass regions. Clearly, the mass model has a significant impact on the r-process path. While the paths up to $N = 116$ are similar, the HFBCS-1 path runs through significantly more neutron-rich nuclei around the $N = 126$ shell closure and beyond. Furthermore, the HFBCS-1 mass model shows gaps before and after the $N = 126$ shell closure, caused by a local rise in neutron separation energy due to deformation effects. This is typical for mass models with strong shell gaps (Kratz et al. 1993; Chen et al. 1995; Pfeiffer et al. 1997) and leads to an underproduction in the final abundances in the corresponding mass region.

Also marked in Figure 1 are the major (contributing more than 1%) progenitor nuclei, as well as their decay paths that feed the α-decay chains responsible for the synthesis of the chronometers ^{232}Th and ^{238}U. This is the mass region where nuclear structure effects can directly affect the predicted U and Th production. Figure 2 shows the nuclear abundances produced in the classical r-process model for both the

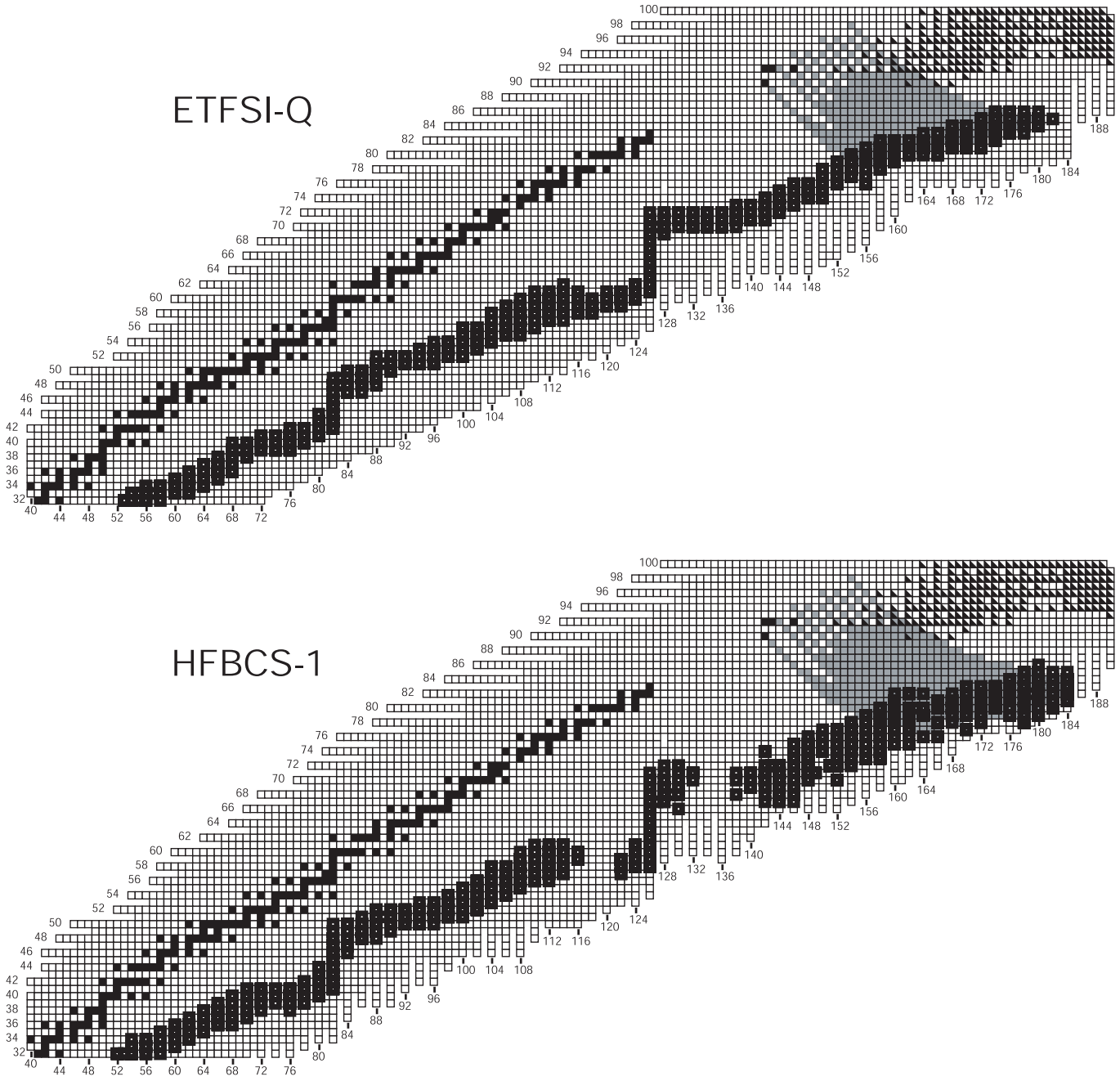

FIG. 1.—The *r*-process path in the classical *r*-process model. The *r*-process waiting points that are progenitors for more than 1% of the final ^{238}U or ^{232}Th abundance are marked as black squares. The decay path from nuclei in the *r*-process into ^{238}U and ^{232}Th is marked with gray squares. Nuclei for which fission after production via β-decay is energetically possible are marked as half-filled squares. The top panel shows the calculation based on the ETFSI-Q mass model and the bottom panel the calculation based on the HFBCS-1 mass model. The charts show only particle-bound nuclei. The neutron drip line has been calculated with the respective mass models.

ETFSI-Q and HFBCS-1 mass models. We display the abundances after β-delayed fission and neutron emission, but before α-decay, to illustrate the impact of different nuclear structure assumptions along the *r*-process paths. Also marked are the nuclei that will α-decay into ^{232}Th or ^{238}U. Figure 2 clearly shows the abundance "trough" before the $N = 184$ shell closure, which is similar to what is found below the $N = 82$ and $N = 126$ shell closures for mass models with strong shell gaps. The $N = 184$ shell gap is somewhat reduced in the ETFSI-Q mass model for nuclei far from stability, but the predicted quenching is not as strong as for the lighter neutron shell gaps (Pearson et al. 1996). Thus, it has no effect on the calculations, as the *r*-process path does not get close enough to the drip line. Therefore, the ETFSI-Q and the HFBCS-1 model calculations yield very similar results.

While the impact of structure effects on the final ^{232}Th and ^{238}U abundances is somewhat reduced by the large number of progenitor nuclei (20 and 15 nuclei, respectively, contribute more than 1% to these species), the steep abundance drop around $A = 240$ in Figure 2 is significant, as the Th progenitors are distributed right across this drop, while

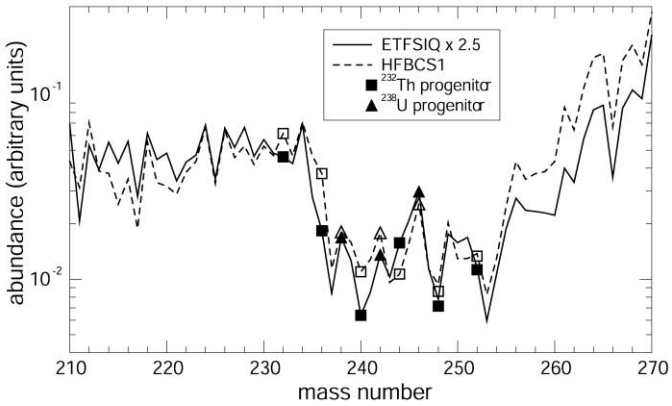

FIG. 2.—Calculated *r*-process abundances after all β-decays (including β-delayed fission) but before α-decays and spontaneous fission. The solid and dashed lines show calculations with the ETFSI-Q and HFBCS-1 mass models, respectively. Also shown are the ETFSI-Q progenitor abundances for ^{232}Th (*filled squares*) and ^{238}U (*filled triangles*), taking into account reduction by spontaneous fission processes. The open symbols are the corresponding progenitors for the HFBCS-1 calculation. For easier comparison, the ETFSI-Q results have been scaled by a factor of 2.5.

the U progenitors are not. The final ^{232}Th/^{238}U ratio is therefore very sensitive to the location of this $A \approx 240$ abundance drop, especially because the $A = 236$ progenitor for ^{232}Th is right on the steep edge. This abundance drop is caused by the rapid change from deformed to spherical nuclei around $N = 163$ along the *r*-process path toward the $N = 184$ shell closure, causing a hump in the neutron separation energies. This effect can be clearly seen in Figures 3 and 4, which show the nuclear deformation and the two-neutron separation energies predicted by the ETFSI-Q mass model for the relevant nuclei. The two-neutron separation energies provide a measure of the neutron separation energies averaged over odd-even effects. As a consequence of the local rise in neutron separation energies toward the neutron drip line, the nuclear abundances produced in the *r*-process are reduced, because it proceeds along constant neutron separation energy contours (see Kratz et al. 1993, Chen et al. 1995, and Pfeiffer et al. 1997 for a discussion of the same effect near the $N = 82$ shell gap). In fact, slight differences between the HFBCS-1 and ETFSI-Q mass models in the

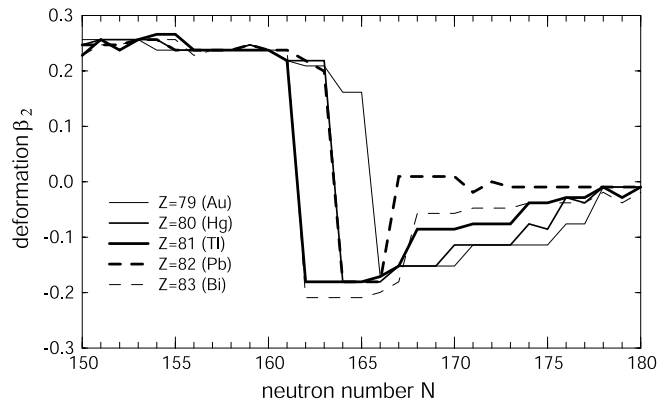

FIG. 3.—Deformation parameter β_2 predicted by the ETFSI-Q mass model as a function of neutron number in the mass region where the *r*-process path crosses the transition from deformed to spherical nuclei. Data are shown for the isotopic chains of Au (*thin solid line*), Hg (*medium solid line*), Tl (*thick solid line*), Pb (*thick dashed line*), and Bi (*thin dashed line*).

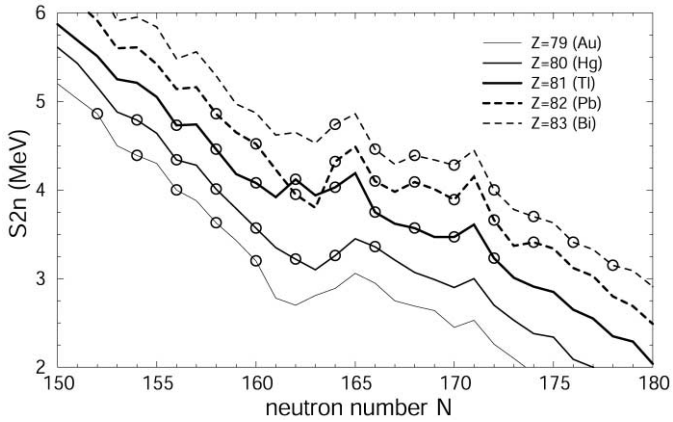

FIG. 4.—Two-neutron separation energies, S_{2n}, predicted by the ETFSI-Q mass model as a function of neutron number in the mass region where the *r*-process path crosses the transition from deformed to spherical nuclei. Line styles as in Fig. 3. Nuclei that are on the classical *r*-process path are marked with circles.

prediction of nuclear shapes for the transition region lead to a slight difference in the location of the predicted abundance drop (Fig. 2). As a consequence, using HFBCS-1, one obtains a higher $A = 236$ production, leading to an enhancement of ^{232}Th over ^{238}U compared to the ETFSI-Q calculations. This leads to a smaller predicted U/Th ratio with HFBCS-1 (0.45, instead of 0.60 with ETFSI-Q), which is the main difference between the two calculations (see Fig. 5).

The *r*-process path, and therefore the possible progenitor nuclei for the synthesis of Th and U, is limited by fission processes. In addition, spontaneous fission can occur in a β-decay chain before an α emitter is reached and can therefore reduce the feeding into the α-decay chains that produce U and Th. To a large extent, the relevant rates are known experimentally. In the ^{238}U production chain, feeding from $A = 250$ is reduced by the 80% fission branch of ^{250}Cm, and for $A = 254$, 258, and 262, known fission branchings close to 100% prevent any contribution. The experimentally known spontaneous fission of the $N = 158$ isotopes from Cf to $Z = 104$ provides an effective barrier that prevents any contribution from $A > 256$ nuclei. In the case of the ^{232}Th production chain, the $A = 248$ contribution is reduced by

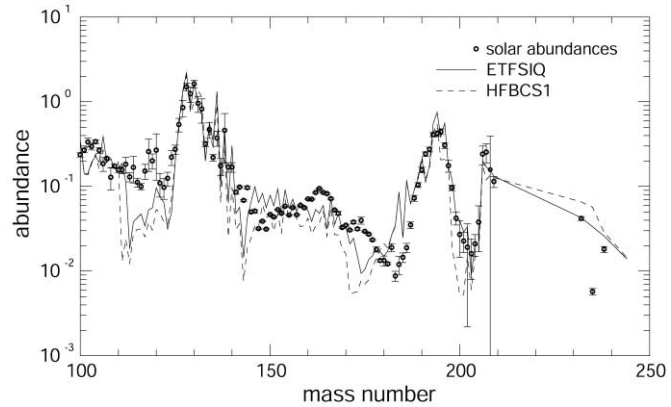

FIG. 5.—Our best fits of the classical *r*-process calculations to the solar system abundance distribution. Shown are the results for the calculations based on the ETFSI-Q (*solid line*) and HFBCS-1 (*dashed line*) mass models.

the 8.39% fission branch of ^{248}Cm. Again, nuclei with $A \geq 256$ cannot contribute, because of the spontaneous fission of $N = 158$ isotopes. For the lighter members of the α-decay chains feeding ^{238}U and ^{232}Th, there is no experimental evidence for losses from spontaneous fission, in agreement with recent theoretical predictions by Goriely & Clerbaux (1999), which are based on the new fission barriers from Mamdouh et al. (1998), also adopted in the present work. The most uncertain case is probably the spontaneous fission rate for the $A = 252$ mass chain. An experimental determination of the fission branching in ^{252}Cm would significantly reduce this uncertainty.

The branchings for neutron-capture–induced fission and β-delayed fission have been estimated based on the fission barriers of Mamdouh et al. (1998). Their fission barrier calculations are based on the same theoretical approach as the ETFSI mass models (Aboussir et al. 1995). By using their fission barriers we ensure consistency in the predictions of Q-values and fission barriers, which is essential to avoid artificial effects from mixing different models (see, e.g., Meyer et al. 1989). We determine fission branchings with the rather simple method of Kodama & Takahashi (1975), one also used by Goriely & Clerbaux (1999). This is a reasonable approach, given the large uncertainties in the fission barriers and Q-values. We find that neutron-induced fission does not play a role along the r-process path leading to the production of ^{238}U and ^{232}Th. However, β-delayed fission is possible for a number of nuclei along the decay chains that connect the r-process paths with the α emitters feeding U and Th (see Fig. 1). In Table 1, we list the corresponding branchings for parent nuclei, based on the same strength functions for allowed and first forbidden decays that were used for the β-decay rate calculations (col. [2]). We assume that fission is always faster than neutron emission. For comparison, Table 1 also lists the branchings obtained only from allowed transitions (col. [3]). Taking into account first forbidden transitions leads only to small corrections. Some of the relevant β-delayed fission branchings have been calculated by Meyer et al. (1989) based on similar strength functions, but using the finite range droplet model (FRDM) for masses, the fission barriers of Howard & Möller (1980), and a significantly more sophisticated barrier penetration formalism. We list their results in Table 1 for comparison (col. [5]), together with data obtained with our method, but using the same masses and fission barriers as in Meyer et al. (1989) (col. [4]). With the exception of ^{252}Np, the predictions based on the same nuclear physics agree quite well, indicating that our simplified approach is in most cases justified. Because the Mamdouh et al. (1998) fission barriers tend to be higher than the ones predicted by Howard & Möller (1980), we conclude that our larger β-delayed fission branchings are most likely a result of the larger β-decay Q-values predicted by ETFSI-Q. On the other hand, Meyer et al. (1989) also found that, in about half of their cases, an improved barrier penetration formalism based on the Wentzel-Kraners-Brillouin (WKB) approximation leads to a substantial reduction in β-delayed fission branchings. Therefore, while β-delayed fission branchings based on the ETFSI-Q mass model and the Mamdouh et al. (1998) fission barriers will be substantially larger than previous estimates, the values given in Table 1 should be regarded as upper limits. This situation is taken into account in the discussion of nuclear physics uncertainties in § 5.

From the above considerations, we find that β-delayed fission is significant and might reduce the final U abundance by up to 10% and the final Th abundance by up to 25%. This is in contrast to previous studies suggesting that β-delayed fission can be neglected completely (Cowan et al. 1991).

TABLE 1

Branchings for β-delayed Fission

Parent Nucleus (1)	GT+FF (%) (2)	GT (%) (3)	H&M (%) (4)	Meyer et al. 1989 (%) (5)
^{252}Ac	3.2	3.2	59	58
^{244}Pa	21	10	...	...
^{246}Pa	13	14	...	...
^{248}Pa	63	77	...	...
^{250}Pa	82	69	15	8
^{252}Pa	61	68	36	36
^{253}Pa	19	12	...	...
^{253}U	6.2	7.2	...	...
^{250}Np	2.5	2.8	...	...
^{252}Np	30	27	37	2

Note.—Col. (2) lists the results of this work taking into account allowed and first forbidden transitions. Col. (3) lists the results we would have obtained with only allowed transitions. Also listed (Col. [5]) are the results from Meyer et al. 1989, based on different nuclear physics and a more sophisticated barrier penetration calculation. Col. (4) lists, for comparison, the results we would have obtained with the same nuclear physics used by Meyer et al. 1989, but with our simplified treatment of the barrier penetration.

4. THE r-PROCESS MODEL PARAMETERS

As a first step, we determine the parameter range of the classical r-process model that fits the solar system r-process abundances (Anders & Grevesse 1989; Arlandini et al. 1999) around the $A = 130$ and 195 abundance peaks, as well as for Pb and Bi (we use here the solar r-process abundances of Cowan et al. 1999). The ability to reproduce the solar ^{206}Pb, ^{207}Pb, ^{208}Pb, and ^{209}Bi abundances is a crucial test of how well our r-process models are able to predict the synthesis of ^{232}Th and ^{238}U, as the r-process fraction of all of these isotopes is predominantly produced from α-decay chains originating in the actinide region. Long-lived (on Galactic chemical evolution timescales) α-decays lead to negligible contributions; Galactic chemical evolution can therefore be neglected when comparing calculated and observed solar Pb and Bi abundances.

These fits have been performed for two sets of nuclear data, differing only in the mass model used to predict neutron separation energies. Figure 5 compares the r-process model predictions obtained with the ETFSI-Q and the HFBCS-1 mass models with the solar r-process abundances. Table 2 list the corresponding r-process model parameters. Both mass models lead to good fits of the major features of the solar system r-process abundance pattern. Most importantly, for ^{206}Pb, ^{207}Pb, ^{208}Pb, and ^{209}Bi, the ETFSI-Q and the HFBCS-1 calculations show excellent agreement with the solar system r-process data (see Fig. 6). For calculations based on ETFSI-Q, this level of agreement has already been demonstrated by Pfeiffer et al. (1997) and Cowan et al. (1999). However, Cowan et al. (1999) also found that calculations based on the ETFSI-1 mass model cannot reproduce the solar Pb and Bi abundances. This problem seems to be solved for the new HFBCS-1 masses.

TABLE 2
CLASSICAL *r*-PROCESS MODEL PARAMETERS

Fit	a_1 (cgs)	a_2 (cgs)	a_3 (cgs)	a_4 (cgs)	T (GK)
ETFSI-Q best fit (Figs. 5, 6, 7).....	3.708432E+04	−1.354975E−01	1.650000E+00	0.000000E+00	1.35
HFBCS-1 best fit (Figs. 5, 6).....	2.270286E+04	−1.393436E−01	4.442493E+01	−6.483987E−02	1.35
Fig. 8, lower dashed line	1.365148E+05	−1.587882E−01	2.841544E+00	−9.719594E−03	1.35
Fig. 8, upper dashed line.....	7.368063E+04	−1.477671E−01	2.157977E+00	−4.799844E−03	1.35
Fig. 8, solid line	3.708432E+04	−1.354975E−01	1.650000E+00	0.000000E+00	1.35
Fig. 8, dot dashed line	1.773023E+04	−1.223097E−01	1.271508E+00	4.648761E−03	1.35

NOTE.—See text (§ 2) for parameter definitions.

A great advantage of Th and U cosmochronometry, based on elemental abundance observations in metal-poor halo stars, is the independence of the results on Galactic chemical evolution models. This is in contrast to methods that compare predictions exclusively with observed solar elemental abundances. Nevertheless, the solar Th and U abundances can provide some limits for *r*-process models that are still largely independent of specific chemical evolution models. We use these constraints here as an additional test of our *r*-process models before we apply them to metal-poor stars.

In essence, one can obtain *r*-process model constraints by using the *r*-process predictions to determine the age of the presolar nebula. This is accomplished by comparing the predicted abundances for ^{232}Th and ^{238}U with the observed solar abundances, corrected for their decay after formation of the solar system. In principle, such an estimate is strongly dependent on the Galactic chemical evolution of *r*-process elements, which is not well understood. However, some largely model-independent constraints can still be obtained. For example, the assumption of a single *r*-process event provides a model-independent lower limit for the age of the presolar nebula. The results for the two mass models are shown in Table 3 (cols. [2] and [4]). None of the calculations yield lower limits that are in conflict with upper limits of the age of the Galaxy at the time of solar system formation. For example, using the cosmological age estimate, derived from high-redshift supernova observations, of $14.9^{+1.4}_{-1.1}$ Gyr (Perlmutter et al. 1999) and an age of the solar system of 4.55 Gyr (Anders & Grevesse 1989), the universe was not older than 11.7 Gyr when the solar system formed. While all our *r*-process models pass this important test, the large spread of the single-event ages from the HFBCS-1 calculations is a problem. Of course, we do not necessarily expect consistent single-event ages, as the entire history of Galactic chemical evolution is surely not characterized by a single burst of elemental enrichment. However, note that the HFBCS-1 calculation predicts a (U/Th) ratio that is essentially identical to the abundance ratio in the presolar nebula, yielding a single-event age close to zero. As any Galactic chemical evolution effects will tend to decrease the U/Th ratio, it will be impossible to find any chemical evolution model that does not yield a U/Th age close to zero when the HFBCS-1 mass model is employed.

In addition, any Galactic chemical evolution model will tend to increase the Th age more than the U and U/Th ages, thus further increasing the spread of ages calculated with the HFBCS-1 model. As an example, Table 3 (cols. [3] and [5]) lists the ages obtained under the assumption of a uniform *r*-process production, which shows indeed a strongly increased inconsistency for the HFBCS-1 ages. Therefore, it will not be possible to find a Galactic chemical evolution model yielding consistent ages of the presolar nebula with the HFBCS-1–based *r*-process model. This conclusion is in agreement with the results from a simple Galactic chemical evolution model (Yokoi, Takahashi, & Arnould 1983), which indicate that solar abundances constrain the *r*-process U/Th ratio to lie within a range of 1.5–2 (Goriely & Arnould 2001). While the HFBCS-1 ratio of 2.2 lies outside of this range, the ETFSI-Q ratio of 1.7 is acceptable. We therefore conclude that the ^{232}Th and ^{238}U abundances predicted by the HFBCS-1 calculations are incompatible with the observed solar system abundances. This leaves the ETFSI-Q–based calculations as the only reasonable choice for *r*-process chronometry in connection with the classical *r*-

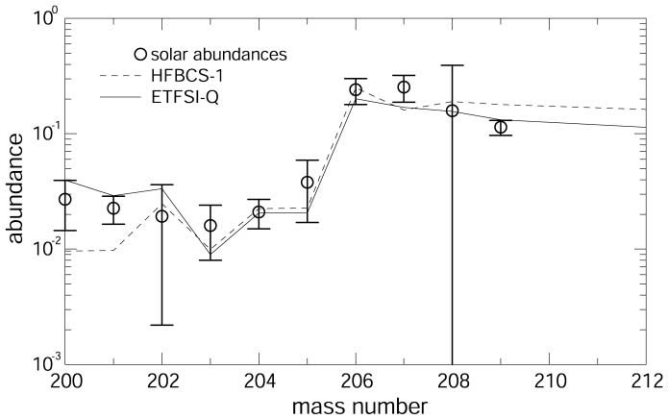

FIG. 6.—Enlargement of a portion of Fig. 5, showing the Pb and Bi region.

TABLE 3
ESTIMATED AGE OF THE PRESOLAR NEBULA

	ETFSI-Q		HFBCS-1	
CHRONOMETER (1)	Single (Gyr) (2)	Uniform (Gyr) (3)	Single (Gyr) (4)	Uniform (Gyr) (5)
U/Th.....	3.2 ± 2.3	7.3 ± 6.3	0.3 ± 2.3	0.8 ± 4.7
U	2.3 ± 1.8	5.0 ± 4.2	4.9 ± 1.8	11 ± 4.9
Th.....	0.3 ± 5.7	1.0 ± 11	14.8 ± 5.7	34 ± 16

NOTE.—Estimates are based on the *r*-process model predictions with two mass models (ETFSI-Q and HFBCS-1) and with two simple assumptions on Galactic chemical evolution: a single event and uniform production.

process model. Figure 7 shows a comparison of elemental abundances from our model predictions with solar *r*-process abundances and the observational data from CS 31082-001. The observed element abundances for $56 \leq Z \leq 77$ are consistent with a solar *r*-process abundance pattern.

5. AGE DETERMINATION AND ERROR ANALYSIS

Absolute ages, τ, for the *r*-process elements in CS 31082-001 can now be determined by comparing the abundance ratios $(U/Th)_0$, $(U/X)_0$, or $(Th/X)_0$, calculated with the classical *r*-process model, with the corresponding observed ratios $(U/Th)_*$, $(U/X)_*$, or $(Th/X)_*$, where X is a stable *r*-process element:

$$\tau = 46.7 \text{ Gyr} \quad \left[\log(\text{Th/X})_0 - \log(\text{Th/X})_*\right], \qquad (1)$$

$$\tau = 14.8 \text{ Gyr} \quad \left[\log(\text{U/X})_0 - \log(\text{U/X})_*\right], \qquad (2)$$

or

$$\tau = 21.8 \text{ Gyr} \quad \left[\log(\text{U/Th})_0 - \log(\text{U/Th})_*\right]. \qquad (3)$$

In the past, Eu ($Z = 63$) has often been chosen as element X. This makes sense for relative age determinations, because Th/Eu ratios are available for a large sample of metal-poor stars, and because Eu is essentially an *r*-only element, making corrections due to *s*-process contaminations in higher metallicity stars unnecessary. However, for an age determination of the *r*-process elements in CS 31082-001, any stable observed element can be used. In fact, for a perfect solar *r*-process pattern in the model predictions and the stellar observations, the result should be independent of the choice of X (Pfeiffer et al. 2001). In this paper, we do not use the *r*-process model predictions for X in the calculation of $(U/X)_0$, but rather the solar abundances $X_\odot$ [therefore, $(U/X)_0 = (U_0/X_\odot)$ and $(Th/X)_0 = (Th_0/X_\odot)$]. This has the advantage that our age estimates become independent of the local deficiencies in the *r*-process model predictions of the stable *r*-process elements X, which are typically much larger than the uncertainties in the solar system abundances. Discrepancies in the estimated ages for different elements X then reflect deviations of the observed stellar abundances from a solar abundance pattern.

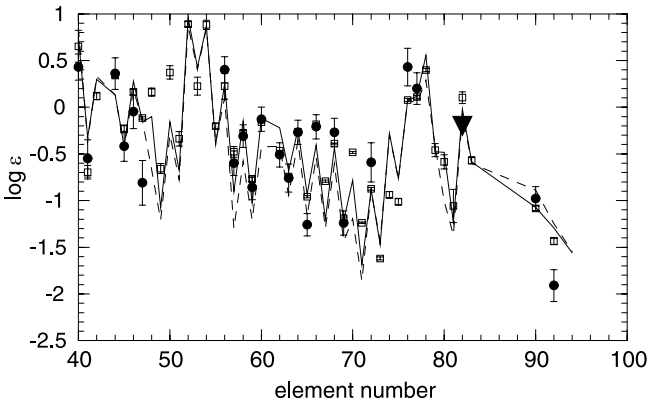

FIG. 7.—Calculated *r*-process elemental abundances for the ETFSI-Q (*solid line*) and the HFBCS-1 (*dashed line*) mass models, compared to the normalized solar abundances (*squares*) and the observed abundances in CS 31082-001 (*circles*). The triangle marks the observed upper limit for Pb in CS 31082-001. All data have been scaled to the $\log \epsilon(\text{X}) = \log_{10}(\text{X/H}) + 12.0$ of the CS 31082-001 observations (X and H are the abundances of element X and hydrogen, respectively).

We have conducted an extensive investigation of the influence of *r*-process model uncertainties on the age determination of CS 31082-001.

1. *β-decay rates.*—The β-decay data used in this work are the same used in Cowan et al. (1999). They represent the only existing data based on updated experimental input and short-range extrapolations (see Kratz et al. 1993 for more details on this technique). To obtain a very conservative estimate of the possible influence of errors in the β-decay data, we performed a Monte Carlo analysis and randomly changed the β-decay half-lives by factors between 0.2 and 5. Branchings for β-delayed neutron emission were also varied. One hundred calculations were then made to determine the variance of the *r*-process abundance predictions. The resulting uncertainty for the logarithmic abundance ratios ranges from ±0.07 for the U/Th ratios to ±0.1 for the U/X and Th/X ratios.

2. *Mass models.*—*R*-process model calculations strongly depend on the choice of mass model. Calculations with a large number of mass models have been done before (Kratz et al. 1993; Chen et al. 1995; Pfeiffer et al. 1997; Kratz et al. 1998; Cowan et al. 1999; Kratz et al. 2000b) and have shown that only the ETFSI-Q mass model can reproduce solar *r*-process abundances, including Pb and Bi, and *simultaneously* give reasonable age values for Th chronometers in metal-poor stars (within the framework of the classical *r*-process model). There are some "hybrid" mass models constructed by mixing predictions from different models for different groups of nuclei, such as the FRDM+Hilf or FRDM+HFB/SkP models discussed in Cowan et al. (1999), that give also reasonable predictions. However, the demand for a consistent, unified nuclear data input (for a discussion, see Kratz et al. 1993) leaves the ETFSI-Q mass model as the only present choice. In this paper we confirm this conclusion, but find that the HFBCS-1 mass model seems to satisfy the same constraints. However, as noted above, the U/Th ratio predicted by the calculations based on the HFBCS-1 mass model is incompatible with the solar system U and Th abundances. As this leaves only one viable mass model, it is difficult to estimate the remaining uncertainties due to mass-model predictions. The huge differences in the abundance predictions of *r*-process model calculations adopting different mass models has been shown extensively before (including the differences between ETFSI-Q and HFBCS-1 calculations in this work). However, it is not so clear what the possible spread in the predicted U and Th abundances is, if one is limited to the subset of mass models that, when used in the classical *r*-process model, fulfill the following three constraints: (1) a reasonable prediction of the distribution of stable *r*-process isotopic abundances from $A = 100$–205, (2) a correct prediction of the solar abundances of Pb and Bi isotopes, mainly produced by α-decay chains from the actinide region, and (3) predicted U and Th abundances that are compatible with the solar U and Th data. A first hint of the total model uncertainties including contributions from the mass model can be obtained by comparing predicted and observed Pb and Bi abundances, and it is discussed below.

3. *Fission processes.*—In this work, we find nonnegligible changes in the predicted Th and U production due to β-delayed fission processes. The resulting changes in the loga-

rithmic abundance ratios are −0.1 for Th/X ratios, −0.05 for U/X ratios, and +0.06 for the U/Th ratio. However, the uncertainties in the predictions of β-delayed fission processes are large. To be conservative, we adopt half of the abundance changes as estimates of their uncertainty, thereby taking into account the possibility of overestimated β-delayed fission branchings.

4. *Model uncertainties*.—We have determined the range of the four classical *r*-process model parameters that still result in a reasonable fit of the solar abundance pattern. Figure 8 shows several calculations covering this parameter range (see Table 2 for the corresponding *r*-process model parameters). Clearly, the U/Th ratio is very robust, making it a more reliable chronometer than the U/X and Th/X ratios, which depend strongly on the *r*-process model parameters. However, so do the predicted Pb and Bi abundances. Limiting the allowed range of *r*-process parameters to models that reproduce solar Pb and Bi abundances, we obtain a model uncertainty for the predicted logarithmic ratios of 0.03 for U/X and Th/X ratios, and 0.002 for U/Th ratios. These errors are quite small, indicating that for a given set of nuclear physics data, the requirement of a reasonable fit of the $A = 195$ peak and good agreement with the Pb abundances (maximum 20% deviation) is a very strong constraint for the *r*-process model parameters.

An independent estimate of the model uncertainties (all sources of error except observational) can be obtained from the deviations between calculated and solar *r*-process abundances of Pb and Bi isotopes. Similar deviations can be expected for the U and Th predictions. On average, we find deviations of only ±0.07 between the calculated and the solar logarithmic abundances. This estimate can be compared with our estimated combined uncertainty from β-decay, fission processes, and model parameters of 0.11 and 0.12 for log (U/X) and log (Th/X), respectively. The average deviation for the predicted logarithmic ratios of Pb and Bi abundances can be used as an estimate for the uncertainty in the prediction of the U/Th ratio. Here we find an error of 0.1, while our estimate from individual sources amounts to 0.08. Overall, our error estimates agree roughly with, or are slightly larger than, the deviations we see in the prediction of Pb and Bi abundances. This indicates that our error estimates are reasonable and do not leave much room for additional uncertainties, for example from nuclear masses.

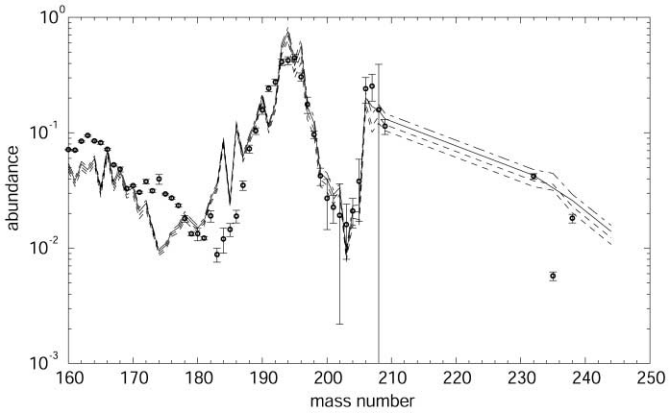

FIG. 8.—Calculations of the *r*-process abundance distribution using the same nuclear physics but varying the parameters of the classical *r*-process model. Each calculation (*line*) has been refitted to the solar *r*-process abundances (*circles*) around the $A = 130$ and $A = 195$ peaks. The solid line is our best fit when Pb and Bi abundances are taken into account. See Table 2 for the corresponding *r*-process model parameters.

Overall, we estimate a total error due to *r*-process model uncertainties (including nuclear physics) of 0.11 for log(U/X), 0.12 for log(Th/X), and 0.10 for log(U/Th). Interestingly, the prediction of the U/Th abundance ratio is not much more reliable than predictions of the Th or U abundances with respect to the solar system distribution of stable nuclei, if Pb and Bi data are taken into account as constraints.

6. RESULTS

Our best predictions of the zero-age abundance ratios and their uncertainties are listed in Table 4 (cols. [2] and [3]) and can now also be applied to other stars. Table 4 also lists the abundance ratios observed in CS 31082-001 (cols. [4] and [5]; Hill et al. 2002). Figure 9 shows all the corresponding U/X, Th/X, and U/Th ages obtained for CS 31082-001. Because we use solar *r*-process abundances for the elements X, the solar system *r*-process abundance pattern for $56 \leq Z \leq 77$ observed in CS 31082-001 is reflected in the excellent agreement among the U/X and Th/X ages. Final U/X and Th/X ages can be determined from a weighted average (based on the uncorrelated fraction of the errors) of all X (see Table 4). However, the resulting U/X (weighted average 7.6 ± 2.3 Gyr), Th/X (weighted average −8.1 ± 5.8 Gyr), and U/Th (15.5 ± 3.2 Gyr) ages clearly do not agree with one another. This shows that our choice of *r*-process model parameters, based on a smooth extrapolation from the solar abundance pattern into the actinide region and reproducing the currently predicted solar Pb *r*-process abundance, is not appropriate for predicting the zero-age U and Th abundances in CS 31082-001 (assuming that a single *r*-process event, or *r*-process events with time intervals that are small compared to the total age, is responsible for the *r*-process enrichment of CS 31082-001).

As already suggested by Cayrel et al. (2001), Goriely & Arnould (2001), and Hill et al. (2002), it is not unreasonable to assume that the prediction of the U/Th ratio produced in the *r*-process is sufficiently robust to be still applicable to CS 31082-001. The main argument for this assumption is the fact that both elements are synthesized from the decay of a large number of progenitor nuclei synthesized by the *r*-process in the same region of the chart of nuclides. With our *r*-process model, this assumption would yield an age estimate for the *r*-process elements in CS 31082-001 of 15 ± 3.2 Gyr. This falls within the age range of 9–18 Gyr given by Goriely & Arnould (2001) for the same star, but based on a different approach.

7. DISCUSSION

Several arguments clearly indicate that standard *r*-process cosmochronometry techniques, based on the assumption of an universal *r*-process abundance pattern for heavy elements, cannot be directly applied to CS 31082-001, because of a peculiar enrichment of Th, and probably also of U.

First, as has been pointed out previously by Truran et al. (2001), Goriely & Arnould (2001), and Hill et al. (2002), the Th/X ratio in CS 31082-001 is about 0.44 dex larger than that observed in CS 22892-052, an otherwise quite similar

TABLE 4
ABUNDANCE RATIOS AND AGES FOR VARIOUS CHRONOMETER PAIRS IN CS 31082-001

Chronometer (1)	*r*-Process Model Ratio (2)	*r*-Process Model Error (3)	CS 31082-001 Ratio (4)	CS 31082-001 Error (5)	Age (Gyr) (6)	Error (Gyr) (7)
log (U/Th)	−0.22	0.10	−0.93	0.11	15.5	3.2
log (U/X) average	...	...	...	...	7.6	2.3
log (U/La)	−0.81	0.12	−1.31	0.12	...	...
log (U/Ce)	−1.01	0.12	−1.60	0.12	...	...
log (U/Pr)	−0.52	0.11	−1.05	0.12	...	...
log (U/Nd)	−1.13	0.11	−1.78	0.12	...	...
log (U/Sm)	−0.83	0.11	−1.40	0.12	...	...
log (U/Eu)	−0.55	0.11	−1.15	0.17	...	...
log (U/Gd)	−1.03	0.11	−1.64	0.13	...	...
log (U/Tb)	−0.33	0.11	−0.66	0.11	...	...
log (U/Dy)	−1.11	0.11	−1.70	0.13	...	...
log (U/Er)	−0.90	0.11	−1.64	0.15	...	...
log (U/Tm)	−0.10	0.11	−0.67	0.14	...	...
log (U/Hf)	−0.42	0.11	−1.32	0.20	...	...
log (U/Os)	−1.37	0.11	−2.35	0.19	...	...
log (U/Ir)	−1.40	0.11	−2.11	0.15	...	...
log (Th/X) average	...	...	...	...	−8.1	5.8
log (Th/La)	−0.60	0.13	−0.38	0.06	...	...
log (Th/Ce)	−0.79	0.13	−0.67	0.04	...	...
log (Th/Pr)	−0.30	0.12	−0.12	0.06	...	...
log (Th/Nd)	−0.91	0.12	−0.85	0.05	...	...
log (Th/Sm)	−0.61	0.12	−0.47	0.06	...	...
log (Th/Eu)	−0.33	0.12	−0.22	0.12	...	...
log (Th/Gd)	−0.81	0.12	−0.71	0.06	...	...
log (Th/Tb)	−0.12	0.12	0.28	0.04	...	...
log (Th/Dy)	−0.89	0.12	−0.77	0.07	...	...
log (Th/Er)	−0.68	0.12	−0.71	0.09	...	...
log (Th/Tm)	0.12	0.12	0.26	0.08	...	...
log (Th/Hf)	−0.20	0.12	−0.39	0.17	...	...
log (Th/Os)	−1.15	0.12	−1.41	0.16	...	...
log (Th/Ir)	−1.18	0.12	−1.18	0.11	...	...

star. Independent of any *r*-process model predictions, this would imply that the *r*-process elements in CS 31082-001 are about 20 ± 10 Gyr (based on Th/Eu) younger than in CS 22892-052, under the assumption that they had the same initial Th/X ratios. Such an age difference between the two stars is clearly incompatible with their (similar) low metallicities (CS 31082-001: [Fe/H] = −2.9; CS 22892-052: [Fe/H] = −3.1) and halo membership. As Hill et al. (2002) point out, these metallicities imply formation within about 1 Gyr after the big bang.

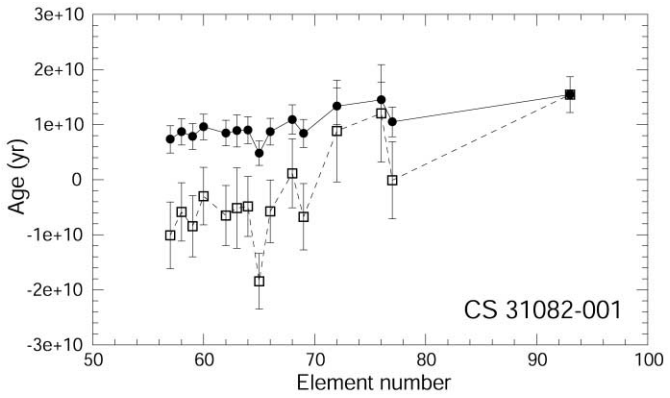

FIG. 9.—Calculated U/X (*solid line*, *circles*) and Th/X (*dashed line*, *open squares*) ages for the *r*-process elements in CS 31082-001 as a function of the element number of X; $Z = 93$ denotes the U/Th age. The error bars include uncertainties in the observed abundances and the uncorrelated errors in the model predictions for U and Th. They are therefore appropriate for a consistency check between U/X and Th/X ages, but not for consistency checks among various U/X ages or among various Th/X ages.

Second, as was immediately realized after the first measurements of the Th abundance in CS 31082-001, absolute Th/X ages based on any reasonable *r*-process model would lead to a very small age. For example, the Th/Eu age based on our *r*-process model prediction would be -5.1 ± 9.3 Gyr.

The only possibility of resolving these problems, while still upholding the principle of a universal *r*-process pattern, would be to assume that the derived very small Th/X ages are correct, but that the *r*-process elements in CS 31082-001 were implanted long after the formation of the star. Indeed, Qian & Wasserburg (2001) speculate that the large enrichment of heavy *r*-process elements in CS 31082-001 can only be explained by exposure of the star to a nearby *r*-process event, for example, the supernova explosion of a companion star. Although repeated radial velocity measurements of CS 31082-001 might rule out the existence of a still-bound companion star (Hill et al. 2002 report stability of the radial velocity for this star at a level of 0.1–0.2 km s^{-1}, albeit over a short baseline of only a year), it cannot be excluded that

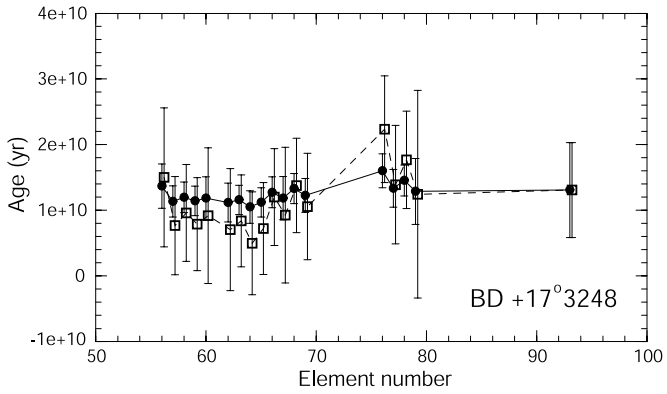

FIG. 10.—Same as Fig. 9, but for BD +17°3248. The Th data points have been slightly shifted to the right to show the overlapping error bars.

the binary system has been disrupted by the supernova explosion.

The difficulty with the above explanation is, as we point out in this paper (see Fig. 9), the inconsistency of the U/X, Th/X, and U/Th ages for the *r*-process elements in CS 31082-001. In principle, this could point to a deficiency in our *r*-process model prediction for U. However, recently the abundance of U has been tentatively determined in a second metal-poor halo star, BD +17°3248 (Cowan et al. 2002). When applying our *r*-process model to this star, we find excellent agreement among the Th/X, U/X, and U/Th ages (see Fig. 10). This suggests that our *r*-process model predictions are not unreasonable and may be applied to other stars.

The most likely conclusion is that CS 31082-001 had a different initial *r*-process abundance distribution than other *r*-process–enhanced, metal-poor, halo stars identified to date. We find that an enhancement of U and Th by a factor of 2.5, compared to our standard *r*-process model, would solve the problems. Figure 11 shows the resulting Th/X, U/X, and Th/U ages. All ages are now consistent with our U/Th age of 15.5 ± 3.2 Gyr, given above. At the same time, the derived Th/X ages would also be in excellent agreement with the estimated ages of other metal-poor stars exhibiting enhanced *r*-process elements, such as CS 22892-052 or HD 115444 (both 15.6 ± 4.6 Gyr; Cowan et al. 1999). It is perhaps suggestive that both problems can be remedied by the proposed initial U and Th enhancement.

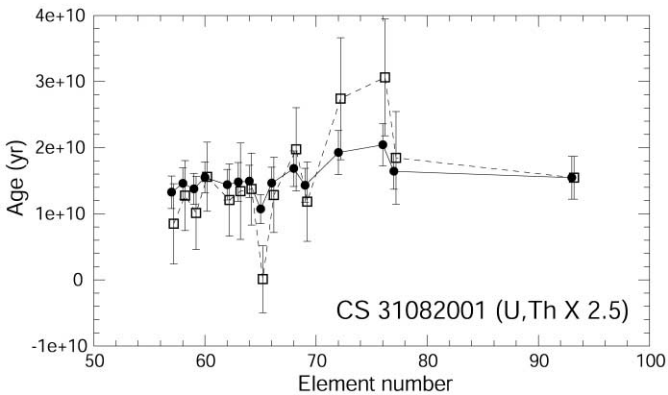

FIG. 11.—Same as Fig. 9, but the zero-age U and Th abundances have been increased by a factor of 2.5. The Th data points have been slightly shifted to the right to show the overlapping error bars.

One way to verify this hypothesis, and to further constrain the zero-age *r*-process abundance distribution, would be to obtain measured abundances of stellar Pb and Bi for one or more of the stars exhibiting *r*-process enhancement. In the case of CS 31082-001, so far only an upper limit for the Pb abundance has been reported (Hill et al. 2002). We can estimate a lower limit of the expected lead abundance in our proposed scenario by assuming that the U and Th enrichment is due to an enhancement of abundances in the $A = 232$–253 region (before α-decay) only. Taking into account Pb production from the decay of U and Th over an age of 15.5 Gyr, we obtain a minimum Pb abundance of $\log \epsilon = +0.16$[6] and a minimum Bi abundance of $\log \epsilon = -0.42$ (50% above our standard prediction for Bi without U/Th enhancement). For Pb, this is more than a factor of 2 above the observed upper limit of $\log \epsilon = -0.2$. However, this problem is mainly due to the large initial Pb abundance produced in our *r*-process model, which had been fitted to agree with the solar *r*-process Pb abundance. Even without any U and Th enhancement, and without any U and Th decays, our predicted initial Pb abundance is already 0.18 dex *above* the observed upper limit. This could be a first observational indication that the *r*-process production of Pb is significantly lower than anticipated. Recent *s*-process calculations that include new experimental data for the ^{208}Pb neutron-capture cross section in fact predict a reduction of the *r*-process contributions to solar Pb by about 0.17 dex (Beer et al. 2001). Because Pb is an important normalization point for our *r*-process model, a reduced *r*-process contribution for Pb would affect our predicted U/X and Th/X ratios and their associated ages. However, it would have a much smaller impact on the U/Th ratio (see Fig. 8).

Turning things around, the amount of Pb synthesized by the decay of the initially enhanced U (^{235}U and ^{238}U) and Th abundances would amount to $\log \epsilon = -0.37$, a factor of 1.5 below the observed upper limit. This can be viewed as a minimum Pb abundance for the proposed age and initial enrichment of CS 31082-001, independent of any direct production of Pb in the *r*-process.

Clearly, measured abundances of Pb and Bi in CS 31082-001 would be extremely important. This would permit us to readjust our *r*-process parameters independently of the estimates for the solar Pb and Bi *r*-process abundances. The element Bi, especially, would play a key role in constraining the initial *r*-process production of the actinides, as Bi originates from a long α-decay chain reaching up to $A = 253$, largely overlapping with the decay chains producing U and Th.

8. SUMMARY AND CONCLUSIONS

Within the context of the classical *r*-process model, we are able to put tighter constraints on the *r*-process production of U and Th. While Pb and Bi are still important calibration points for the model, they are not the only data points constraining the U and Th abundance pattern. This is an advantage over the multievent canonical *r*-process model.

[6] All abundances are given in the standard notation, $\log \epsilon(\mathrm{X}) = \log_{10}(\mathrm{X/H}) + 12.0$, and have been scaled to the CS 31082-001 observations (X and H are the abundances of element X and hydrogen, respectively).

One important difference, with respect to other recent calculations, is the nonnegligible impact of β-delayed fission on the Th and U production in the *r*-process. Using a self-consistent approach with the new fission barriers of Mamdouh et al. (1998) and the ETFSI-Q mass model, we find that β-delayed fission can change Th/X ages by up to 4.6 Gyr, U/X ages by up to 0.7 Gyr, and U/Th ages by up to 1 Gyr.

In this work we use, for the first time, the HFBCS-1 mass model for *r*-process cosmochronometry within the framework of the classical *r*-process model. We find that calculations based on HFBCS-1 masses do indeed fit the solar Pb and Bi abundances, which had been a problem with the ETFSI-1 mass model (Pfeiffer et al. 1997; Cowan et al. 1999). However, because of a slightly different prediction of the onset of deformation effects in the Hg-Pb region around $N = 163$, before the $N = 184$ shell gap, the HFBCS-1 calculations predict a relatively high Th production that is inconsistent with solar U and Th data. We therefore use the ETFSI-Q mass model throughout this work.

Overall, our predicted abundance ratios are in agreement with previous estimates. For example, our log(Th/Eu) ratio is -0.33 ± 0.12, which agrees within errors with the ratios found by Cowan et al. (1999; -0.32) and Goriely & Clerbaux (1999; -0.31) using the same mass model. However, these authors used purely theoretical Th/Eu ratios, while we use the ratio of calculated Th abundance to solar (*r*-process) Eu abundance. The latter is independent of uncertainties in the *r*-process model predictions in the Eu region.

In this paper, we have chosen a somewhat conservative approach in estimating the model uncertainties. For example, our estimates for the model uncertainty in the predicted log(Th/Eu) ratio is 0.12, while Cowan et al. (1999) estimate 0.06. Indeed, our predictions for the log(U/Th) ratio of -0.22 ± 0.1 include the whole range of predictions listed in Cowan et al. (1991; -0.28 to -0.15), spanning more than 20 years of work from various authors. However, it is significantly narrower than the range of predictions given in Goriely & Clerbaux (1999) for calculations with different nuclear physics assumptions (-0.22 to $+0.05$). Some of the predictions in Goriely & Clerbaux (1999) are based on nuclear physics models that have been demonstrated to be unsuitable for the prediction of U and Th production in the *r*-process. However, their value for log(U/Th), based on the ETFSI-Q mass model, is -0.22, which agrees exactly with our prediction.

Observational errors associated with the determination of elemental abundances for CS 31082-001 exceed our estimates of the *r*-process model uncertainties for most species (see Table 4), even though they are based on arguably some of the best high-resolution data ever obtained for an extremely metal-poor star (S/N $>$ 500 per resolution element). In the future, more accurate abundance measurements and stellar model atmospheres would therefore lead to significantly improved age estimates. Even with our current, conservative error estimates, *r*-process cosmochronometry is a promising method for the determination of absolute ages of the *r*-process elements in very metal-poor stars. Our pure *r*-process model-induced uncertainties result in age uncertainties of 5.6 Gyr for Th/X ages, 1.6 Gyr for U/X ages, and 2.2 Gyr for U/Th ages for this method. Improvements in our understanding of the properties of very neutron-rich nuclei are necessary to go beyond these limits. More reliable calculations of β-delayed fission processes would be especially important. Clearly, an identification of the *r*-process site and more realistic *r*-process models would also be important to verify the assumptions underlying the classical *r*-process model.

We find that standard chronometry techniques, based on a smooth extrapolation of solar *r*-process abundances using the classical *r*-process model, cannot be applied to CS 31082-001. Our most likely explanation is that U and Th in the *r*-process debris incorporated in CS 31082-001 during its formation were enhanced by about a factor of 2.5 over the standard predictions. If we assume that this enhancement does not affect the U/Th ratio produced in the *r*-process, we find an age of 15.5 ± 3.2 Gyr for the *r*-process elements in CS 31082-001. This is consistent with recent estimates for the age of the universe, from high-redshift supernova observations, of $14.9^{+1.4}_{-1.1}$ Gyr (Perlmutter et al. 1999) and a formation of CS 31082-001 within $\approx$1 Gyr after the big bang.

A long-standing question is whether *r*-process events produce a universal *r*-process abundance pattern. There is very strong evidence, from abundance measurements in a number of very metal-poor stars, that such a pattern exists for elements with $56 \leq Z \leq 76$. Most recently, Johnson & Bolte (2001) compared observed abundances of 22 metal-poor stars and found agreement with the solar system *r*-process abundance pattern within uncertainties. As Hill et al. (2002) and Figure 7 in this paper show, this is also true for CS 31082-001. Therefore, all *r*-process–enhanced, metal-poor stars found to date exhibit the same solar *r*-process abundance pattern for elements with $56 \leq Z \leq 76$.

The important question for *r*-process cosmochronometry is whether this pattern extends (for zero age) to U and Th and whether it can be reliably predicted by a smooth extrapolation based on the classical *r*-process model. While this is not the case for CS 31082-001, there is evidence that this assumption is valid for most of the *r*-process–enhanced stars found so far. Most importantly, application of our U and Th predictions to BD $+17^{\circ}3248$, the only other star with a measured U abundance, indeed leads to consistent U/X, Th/X, and U/Th ages. In addition, Th/Eu ages derived from our *r*-process model predictions for the six remaining *r*-process–enhanced, very metal-poor stars in which a Th abundance has been determined span a reasonable range from 8 to 17 Gyr. Especially, the very small dispersion of the observed Th/Eu ratio in four of those stars (Johnson & Bolte 2001) points to a consistent *r*-process abundance pattern that extends to the actinides, although, of course, real age differences could be present. We therefore conclude that the assumption of a "universal" *r*-process abundance pattern reaching into the actinide region likely is valid in most cases and that CS 31082-001 is an exception. Hence, *r*-process cosmochronometry remains a powerful tool to obtain constraints on the age of the Galaxy and on the history of the chemical evolution of *r*-process elements in the Galaxy.

However, a remaining complication for cosmochronometry is the reliable identification of stars in which the zero-age abundance pattern for U and Th deviates from the standard. This will be especially difficult in cases for which the deviations are small enough to give still "reasonable" age estimates. In the case of CS 31082-001, deviations could be determined from the inconsistency of U/X, Th/X, and U/Th ages. Future Pb or Bi abundance observations in CS 31082-001 should provide critical information on whether these elements can be used to derive reliable criteria on how to determine the zero-age U and Th abundances. For CS

31082-001, we predict a lower limit for the Pb abundance of $\log \epsilon = -0.37$, only 0.17 dex below the current observational upper limit, if the proposed scenario of an initial enrichment in U and Th and an age of 15.3 Gyr is correct.

While the exceptional enrichment of U and Th in CS 31082-001, together with a standard *r*-process abundance pattern for the majority of the other stable elements, represents a complication for cosmochronometry, it might provide important clues on the nature of the *r*-process itself. In fact, how such a selective enhancement of the actinides can occur in an *r*-process event remains an interesting open question. The $N = 126$ shell closure acts as the last bottleneck in the *r*-matter flow to the actinide region. From the nuclear physics input, the description of the $A = 195$ peak region turns out to be surprisingly robust, thus providing tight constraints for its full buildup and the correlated acceleration of the *r*-process beyond $N = 126$ toward the $230 < A < 250$ region containing the (main) progenitors of Th and U. Therefore, from these rather straightforward arguments, a selective accumulation of material in the actinide region between the $N = 126$ and 184 shell closures during the *r*-process seems to be almost impossible to achieve from a nuclear structure point of view.

Future discoveries of more halo stars with similar metallicity and *r*-process enrichment levels and measurable abundances of both U and Th is a clear necessity. This will permit the establishment of a more complete picture of the variations of the *r*-process production of U and Th over the early history of the Galaxy. Dedicated observational programs to accomplish these goals are already underway (following the approach outlined by Christlieb et al. 2001), so there is hope of progress in the near future.

This work was carried out under NSF contracts PHY 00-72636 (Joint Institute for Nuclear Astrophysics, JINA) and PHY 95-28844. H. S. is an Alfred P. Sloan fellow. K.-L. K. and B. P. acknowledge support through the German BMBF, grant 06 MZ 9631. T. C. B. acknowledges partial support of this work from grants AST 00-98508 and AST 00-98549 from the US National Science Foundation. J. C. was supported by NSF grant AST 99-86974.

REFERENCES

Aboussir, Y., Pearson, J. M., Dutta, A. K., & Tondeur, F. 1995, At. Data Nucl. Data Tables, 61, 127
Anders, E., & Grevesse, N. 1989, Geochim. Cosmochim. Acta, 53, 197
Arlandini, C., Käppeler, F., Wisshak, K., Gallino, R., Lugaro, M., Busso, M., & Straniero, O. 1999, ApJ, 525, 886
Beer, H., Rochow, W., Mutti, P., Corvi, F., Kratz, K.-L., & Pfeiffer, B. 2001, in Structure of the Nucleus at the Dawn of the Century, ed. G. C. Bonsignori, M. Bruno, A. Ventura, & D. Vretenar (Singapore: World Scientific), 372
Burris, D. L., Pilachowski, C. A., Armandroff, T. E., Sneden, C., Cowan, J. J., & Roe, H. 2000, ApJ, 544, 302
Butcher, H. R. 1987, Nature, 328, 127
Cayrel, R., et al. 2001, Nature, 409, 691
Chen, B., Dobaczewski, J., Kratz, K.-L., Langanke, K., Pfeiffer, B., Thielemann, F.-K., & Vogel, P. 1995, Phys. Lett. B, 355, 37
Christlieb, N., et al. 2001, in ASP Conf. Ser. 245, Astrophysical Ages and Time Scales, ed. T. von Hippel, C. Simpson, & N. Manset (San Francisco: ASP), 298
Cowan, J. J., Burris, D. L., Sneden, C., McWilliam, A., & Preston, G. W. 1995, ApJ, 439, L51
Cowan, J. J., McWilliam, A., Sneden, C., & Burris, D. L. 1997, ApJ, 480, 246
Cowan, J. J., Pfeiffer, B., Kratz, K.-L., Thielemann, F.-K., Sneden, C., Burles, S., Tytler, D., & Beers, T. C. 1999, ApJ, 521, 194
Cowan, J. J., Thielemann, F.-K., & Truran, J. 1991, Phys. Rep., 208, 267
Cowan, J. J., et al. 2002, ApJ, 572, 861
Cowley, C. R., Allen, M. S., & Aikman, G. C. L. 1975, Nature, 258, 311
Dobaczewski, J., Nazarewicz, W., & Werner, T. R. 1995, Phys. Scr. T 56, 15
François, P., Spite, M., & Spite, F. 1993, A&A, 274, 821
Freiburghaus, C., Rembges, J.-F., Rauscher, T., Kolbe, E., Thielemann, F.-K., Kratz, K.-L., Pfeiffer, B., & Cowan, J. J. 1999, ApJ, 516, 381
Goriely, S., & Arnould, M. 2001, A&A, 379, 1113
Goriely, S., & Clerbaux, B. 1999, A&A, 346, 798
Goriely, S., Tondeur, F., & Pearson, J. M. 2001, At. Data Nucl. Data Tables, 77, 311
Hill, V., Plez, B., Cayrel, R., & Beers, T. C. 2001, in ASP Conf. Ser. 245, Astrophysical Ages and Time Scales, ed. T. von Hippel, C. Simpson, & N. Manset (San Francisco: ASP), 316
Hill, V., et al. 2002, A&A, 387, 560
Howard, W. M., & Möller, P. 1980, At. Data Nucl. Data Tables, 25, 219
Johnson, J. A., & Bolte, M. 2001, ApJ, 554, 888
Kodama, T., & Takahashi, K. 1975, Nucl. Phys. A, 239, 489
Kratz, K.-L., Bitouzet, J.-P., Thielemann, F.-K., Möller, P., & Pfeiffer, B. 1993, ApJ, 403, 216
Kratz, K.-L., Möller, P., Pfeiffer, B., & Thielemann, F.-K. 2000a, in Origin of Elements in the Solar System: Implications of Post-1957 Observations, ed. O. Manuel (New York: Kluwer/Plenum), 119
Kratz, K.-L., Pfeiffer, B., & Thielemann, F.-K. 1998, Nucl. Phys. A, 630, 352
Kratz, K.-L., Pfeiffer, B., Thielemann, F.-K., & Walters, W. B. 2000b, Hyperfine Interact., 129, 185
Mamdouh, A., Pearson, J. M., Rayet, M., & Tondeur, F. 1998, Nucl. Phys. A, 644, 389
Mathews, G. J., & Cowan, J. J. 1990, Nature, 345, 491
McWilliam, A., Preston, G. W., Sneden, C., & Searle, L. 1995a, AJ, 109, 2757
McWilliam, A., Preston, G. W., Sneden, C., & Shectman, S. 1995b, AJ, 109, 2736
Meyer, B. S., Howard, W. M., Mathews, G. J., Takahashi, K., Möller, P., & Leander, G. A. 1989, Phys. Rev. C, 39, 1876
Meyer, B. S., & Truran, J. W. 2000, Phys. Rep., 333, 1
Möller, P., Nix, J. R., & Kratz, K.-L. 1997, At. Data Nucl. Data Tables, 66, 131
Pearson, J. M., Nayak, R. C., & Goriely, S. 1996, Phys. Lett. B, 387, 455
Perlmutter, S., et al. 1999, ApJ, 517, 565
Pfeiffer, B., Kratz, K.-L., & Thielemann, F.-K. 1997, Z. Phys. A, 357, 235
Pfeiffer, B., Kratz, K.-L., Thielemann, F.-K., & Walters, W. B. 2001, Nucl. Phys. A, 693, 282
Qian, Y.-Z., & Wasserburg, G. J. 2001, ApJ, 552, L55
Sneden, C., Cowan. J. J., Ivans, I. I., Fuller, G. M., Burles, S., Beers, T. C., & Lawler, J. E. 2000a, ApJ, 533, L139
Sneden, C., Johnson, J., Kraft, R. P., Smith, G. H., Cowan, J. J., & Bolte, M. S. 2000b, ApJ, 536, L85
Sneden, C., McWilliam, A., Preston, G. W., Cowan, J. J., Burris, D. L., & Armosky, B. J. 1996, ApJ, 467, 819
Sneden, C., Preston, G. W., McWilliam, A., & Searle, L. 1994, ApJ, 431, L27
Spite, M., & Spite, F. 1978, A&A, 67, 23
Takahashi, K., Yamada, M., & Kondoh, T. 1973, At. Data Nucl. Data Tables, 12, 101
Truran, J. W., Burles, S., Cowan, J. J., & Sneden, C. 2001, in ASP Conf. Ser. 245, Astrophysical Ages and Time Scales, ed. T. von Hippel, C. Simpson, & N. Manset (San Francisco: ASP), 226
Westin, J., Sneden, C., Gustafsson, B., & Cowan, J. J. 2000, ApJ, 530, 783
Yokoi, K., Takahashi, K., & Arnould, M. 1983, A&A, 117, 65